Published in final edited form as:
Math Biosci. 2009 January ; 217(1): 19–26. doi:10.1016/j.mbs.2008.10.002.

A Simple Mathematical Model of Signaling Resulting from the Binding of Lipopolysaccharide with Toll-like Receptor 4 Demonstrates Inherent Preconditioning Behavior

Beatrice Rivière[¶,§], **Yekaterina Epshteyn**[¶,#], **David Swigon**[¶,§], and **Yoram Vodovotz**[*,§,†]

¶ *Department of Mathematics, University of Pittsburgh, Pittsburgh, PA 15261*

* *Department of Surgery, University of Pittsburgh, Pittsburgh, PA 15213*

§ *Center for Inflammation and Regenerative Modeling, McGowan Institute for Regenerative Medicine, University of Pittsburgh, Pittsburgh, PA 15219*

Abstract

The complex biology of Gram-negative bacterial lipopolysaccharide (LPS) is central to the acute inflammatory response in sepsis and related diseases. Repeated treatment with LPS can lead to desensitization or enhancement of subsequent responses both *in vitro* and *in vivo* (a phenomenon known as preconditioning). Previous computational studies have demonstrated a role for anti-inflammatory influences in this process (Day et al, J. Theor. Biol. 2006. 242:237). Since LPS signals via Toll-like receptor 4 (TLR4), we created a simple mathematical model in order to address the role of this receptor in both the normal and preconditioned response to LPS. We created a nonlinear system of ordinary differential equations, consisting of free LPS, free TLR4, bound complex LPS-TLR4, and an intracellular signaling cascade (lumped into a single variable). We simulate the effects of preconditioning by small and large repeated doses of LPS on the system, varying the timing of the doses as well as the rate of expression of TLR4. Our simulations suggest that a simplified model of LPS/TLR4 signaling can account for complex preconditioning phenomena without invoking a specific signaling inhibition mechanism, but rather based on the dynamics of the signaling response itself, as well as the timing and magnitude of the LPS stimuli.

Keywords

inflammation; mathematical model; sepsis; preconditioning; lipopolysaccharide; endotoxin; tolerance

INTRODUCTION

The inflammatory response (local or systemic) is a highly complex process that involves innumerous cell types and mediators that act in concert in order to eradicate infection and promote tissue repair. This response is characterized by both context-dependent phenomena

†To whom correspondence should be addressed at: Department of Surgery, University of Pittsburgh, W944 Biomedical Sciences Tower, 200 Lothrop St., Pittsburgh, PA 15213, Tel.: 412-647-5609, Fax: 412-383-5946, E-mail: vodovotzy@upmc.edu.
[#]Current address: Department of Mathematical Sciences, Carnegie Mellon University, Pittsburgh, PA 15213

and by an array of control processes [25]. We have created a series of mathematical models of the inflammatory response and its links to tissue damage and healing [2;33;34]. One of the aspects of inflammation that we have been studying involves preconditioning [9], a phenomenon in which secondary inflammatory stimulation (with either the same or different pro-inflammatory agent or stress) leads to one of three possible outcomes with regard to a single pro-inflammatory stimulus [6;37]:

1. No difference, i.e. both the first and second responses are of the same magnitude;
2. Priming, in which the second response is greater than the first; or
3. Desensitization (tolerance), in which the second response is lower than the first.

Repeated treatment with Gram-negative bacterial lipopolysaccharide (LPS) is a well-established paradigm of preconditioning. Previous computational studies from our group, using a lumped-parameter model, have demonstrated a role for anti-inflammatory influences in this process at the whole-animal levels [9]. There is abundant evidence that preconditioning occurs at the cellular level as well as *in vivo* [6;37]. Lipopolysaccharide signals via Toll-like receptor 4 (TLR4) [4;20], and desensitization in response to LPS has been associated with suppression of TLR4 signaling [13]. To gain insight into this process, we created a simple mathematical model TLR4 signaling in both the normal and preconditioned responses of macrophages to LPS. These studies demonstrate computationally how various, often subtle features of LPS-driven preconditioning could occur at the cellular level, without invoking any overt anti-inflammatory influences.

MATERIALS AND METHODS

A mathematical model of signaling

The mathematical model consists of a system of ordinary differential equations containing LPS (A), TLR4 (R), the bound complex LPS-TLR4 (C), and downstream signaling carrier (S):

$$\begin{aligned}
\frac{dA}{dt} &= -k_1 AR + k_{-1} C \\
\frac{dR}{dt} &= -k_1 AR + k_{-1} C + k_2 \left(1 - \frac{R}{r_0}\right) \\
\frac{dC}{dt} &= k_1 AR - k_{-1} C - k_3 \chi_{C \geq c_0} (C - c_0)^2 \\
\frac{dS}{dt} &= k_4 (C - S)
\end{aligned}$$

These equations describe the dynamics of R and C on the surface of cells, A in the vicinity of the surface and S in the cell interior. LPS binds to TLR4 with a rate k_1 to form an LPS-TLR4 complex, which can dissociate with a small rate k_{-1} [31], or can be internalized by the cell at a rate k_3. We have not included a decay mechanism for LPS, as LPS is known to be intrinsically stable with a negligible death rate (see [14;17]. TLR4 is expressed by cells at a constant rate k_2 and, in the absence of LPS, it equals to the homeostatic value r_0. The LPS-TLR4 complex stimulates signaling cascade at a rate k_4. The last term in the equation for LPS-TLR4 complex accounts for the existence of a threshold value c_0 under which internalization of the complex does not occur; the step function $\chi_{C \geq c0}$ takes the value 1 if $C \geq c_0$ and the value 0 otherwise. The initial amounts are assumed zero for both complex and signaling cascade, r_0 for the free receptors, and a constant prescribed value for LPS. The time interval is subdivided into several subintervals. The strong-stability preserving Runge-Kutta method of third order is used to solve the ODE system numerically at each time step for each cell. The parameter values used in the model are shown in Table I.

RESULTS

Analysis of the system

We first analyze the stability of the ODE system in the case of $k_{-1} = 0$. The first two equations are independent of the *S* and *C* variables and hence form a closed system. The phase portrait for the *A*–*R* system (not shown) has an asymptotically stable fixed point at $(A, R) = (0, r_0)$. Trajectories originating at $R = r_0$ are monotone decreasing in *A* with a decrease followed by an increase in *R*. The product *AR* is positive and converges to 0, which results in a positive, but finite, contribution to *C*. The third equation then implies that if the integral $J=\int_0^\infty k_1 AR dt$ is less than c_0, *C* will approach the value *J* monotonically, as $t \to \infty$. Otherwise, the *C* trajectory will show a peak and then decay to c_0 (see Figure 7).

When $k_{-1} > 0$, the equations for *A*, *R*, and *C* are again independent of *S*. The phase portrait for the *A*-*R*-*C* system (not shown) has a line of fixed points $(A, R, C) = (A, r_0, Ak_1r_0/k_{-1})$ with $0 \leq A \leq k_{-1}c_0/(k_1r_0)$. For the parameters listed in Table 1 these fixed points are neutrally stable, i.e., have one zero eigenvalue and two real negative eigenvalues.

The last equation implies that the signaling *S* is determined by the dynamics of *C*:

$$S(t)=S(0)e^{-k_4 t}+k_4\int_0^t C(t)e^{-k_4(t-\tau)}d\tau$$

In other words, the effect of initial value *S*(0) is lost on the timescale of $1/k_4$ and the value of *S* at time *t* is the average of *C* over an interval of time terminating at *t* of length of the order of $1/k_4$. As a result, if k_4 is sufficiently large, the dynamics of *S* is almost identical to that of *C*.

In the standard trajectory corresponding to the initial conditions $(A, R, C, S) = (A, r_0, 0, 0)$ with constants as given by Table I, the amount of *A* is monotonically decreasing, *R* shows initial decrease, followed by an increase back to $R = r_0$, and both *C* and *S* show an increase with a single peak, followed by a decrease to very small levels. We shall now examine several distinct preconditioning scenarios.

Scenario 1

We show simulations of two successive injections of LPS done at a time interval Δt apart. The curves in panel A show the amount of signaling (vertical axis) versus the time (horizontal axis). Solid lines correspond to a small interval between the two LPS injections (Δt = 10h) whereas dotted lines correspond to a large interval between the two injections (Δt = 40h). We vary the amount of LPS for each injection. For panel A and panel B, two large and equal amounts of LPS were injected (A(t=0)=A(t= Δt)=10); for panel C and panel D, one large amount was first injected (A(t=0)=10), then followed by a small amount (A(t=Δt)=1); for panel E and panel F, two small and equal amounts of LPS were injected (A(t=0)=A(t=Δt)=1) and finally for panel G and panel H a small amount was first injected (A(t=0)=1) then followed by a large amount (A(t=Δt)=10). The parameters in the mathematical model are given in Table I. Panels A, C, E and G correspond to the regeneration rate of TLR4 rate equal to 0.5 whereas panels B, D, F and H correspond to a smaller regeneration rate (equal to 0.1).

We first observe that decreasing the regeneration rate of TLR4 has a direct effect on the second signaling peak for panels A and B. For a rate equal to 0.5, we observe tolerance if Δt is small enough between the two stimuli and we have two signaling peaks of the same magnitude if Δt is large enough. For a rate equal to 0.1, we only observe an important desensitization. If the

second LPS stimulus is smaller than the first (panel C and D), we observe a smaller second signaling peak if the rate is equal to 0.5, and no second peak at all if the rate is equal to 0.1.

For panels E, F, G and H, we obtain priming, namely the second peak is larger than the first signaling peak. For the case where the same small amount of LPS is injected, we do observe a larger priming if the interval Δt is small enough. This effect does not appear if the second LPS stimulus is larger than the first stimulus: the magnitude of the second signaling peak seems to be independent of Δt.

Scenarios 2–6

The general description of scenarios 2–6 is found in Table 2, and are based on the canonical preconditioning scenarios described by Day *et al* [9]. We use the same parameters as in Table I and regeneration rate of TLR4 equal to 0.1.

Scenario 2—(see Figure 2A). In the non-preconditioned system, only one signaling peak occurs following a single LPS injection at time t=24h. The system is next preconditioned by injecting a small amount of LPS at the initial time (scenario 2a and 2b). This produces two signaling peaks of different magnitude. The peak following the initial injection is smaller than the peak following the second stimulus. If the initial amount of LPS is increased and equal to one (scenario 2a), the second signaling peak is only slightly smaller than the peak obtained in the non-preconditioned system. If the initial amount is three times larger (scenario 2b), there is a significant decrease in the magnitude of the second signaling peak compared to the non-preconditioned system. There is still a small difference between the magnitude of the first and second peaks. Figure 2B shows that the magnitude S_{max} of the second peak decreases approximately linearly with the increase in preconditioning, until a threshold is reached beyond which no further decrease in signaling through preconditioning is achievable. This threshold occurs for $A(t=0) \sim 7$. We also note that the signaling amount does not go to zero, but remains slightly elevated and equal to 0.7.

We conclude that by preconditioning the system with a low dose of LPS, one can reduce the response obtained with a very large dose of LPS.

Scenario 3—(see Figure 3A). This scenario follows a similar pattern as in scenario 2. The non-preconditioned system gives a single signaling peak following the LPS stimulus at t=26h. Then, the system is preconditioned by injecting increasing amounts of LPS at time t=0. This gives two successive signaling peaks (scenarios 3a, 3b, 3c). As the initial amount of LPS increases from 1 (scenario 3a) to 2 (scenario 3b) and then to 3 (scenario 3c), the magnitude of the first peak increases and the magnitude of the second peak decreases. In fact, for a preconditioning amount equal to 3, the first and second peaks have the same magnitude. This differs from scenario 2, where a small difference between the two peaks was still observed. An explanation for this difference is that the amount of LPS in the non-preconditioned system in scenario 3 is half the amount of LPS in scenario 2 (namely 5 versus 10). In scenario 3, the amount is less lethal and the magnitude of the second peak is smaller than the one in scenario 2. Another difference between the results in scenario 2 and scenario 3 is that the tail of the signaling peak is smaller in scenario 3 than in scenario 2. In scenario 3, at t=80h, signaling peaks at an amount of 0.2, whereas in scenario 2 signaling peaks at an amount of 0.7. Again, this can be explained by a smaller LPS stimulus in scenario 3. Figure 3B shows that again the magnitude S_{max} of the second peak decreases approximately linearly with the increase in preconditioning until a threshold $A(t=0) \sim 7$ is reached beyond which no further decrease in signaling through preconditioning is achievable.

We conclude that preconditioning helps decrease the magnitude of the signaling peak but it also creates a “tail” in the signaling evolution. As the amount of preconditioning increases, it

takes longer for the system to go back to its normal state, i.e. for the signaling amount to become close to zero.

Scenario 4—(see Figure 4). We consider three different systems with and without preconditioning. The amount of LPS is identical in all non-preconditioned systems. Panel A shows a non-preconditioned system with a single LPS injection at time t=24h (solid line) and a preconditioned system with an initial LPS stimulus equal to 2 (dashed line). In the preconditioned system, there are two signaling peaks. The second signaling peak shows a reduction of 16% compared to the peak in the non-preconditioned system. Panel B shows a non-preconditioned system with a single LPS stimulus at a later time t=48h (solid line) and a preconditioned system with two LPS injections of an amount equal to 2 each at times t=0h and t=24h (dashed line). The resulting signaling curve shows three signaling peaks. The magnitude of the third peak is 25% smaller than the magnitude of the signaling peak in the non-preconditioned system. Panel C shows a non-preconditioned system with a single LPS injection at time t=72h (solid line) and a preconditioned system with three LPS stimuli at successive times t=0h, t=24h and t=48h. This produces four signaling peaks with a reduction of 30% for the last peak compared to the non-preconditioned peak. We observe that in all three panels, the signaling peak following the LPS injection in the non-preconditioned systems is identical, namely independent of the injection time. We also observe that for all preconditioned systems, the first LPS peak is identical. This is expected as the same amount of LPS is injected at the same initial time. Also, the second signaling peak in panel B is identical to the second signaling peak in panel C.

We conclude that several successive preconditioning stimuli help reduce the system's response to a large amount of LPS.

Scenario 5—(see Figure 5). In this scenario, the non-preconditioned system has a very large and lethal amount of LPS injected at t=72h. The amount is equal to 15. This results in a high signaling peak following the injection (solid line). Next, we consider two types of preconditioning. In scenario 5a, two LPS injections of an equal amount of 2 occur at t=0 and t=24h. This produces three signaling peaks (dotted line). The third signaling peak is 23% smaller compared to the non-preconditioned peak. In scenario 5b, three LPS injections occur at times t=0, t=24h and t=48h with a smaller amount equal to 1 (dashed line). The resulting fourth signaling peak around t=72h is 16% lower than the non-preconditioned peak.

From this simulation, we conclude that a better preconditioning strategy is fewer successive LPS stimuli of small amount rather than more successive LPS stimuli of very small amount.

Scenario 6—(see Figure 6A). This scenario is of the same type as scenario 2. The non-preconditioned system has a larger LPS injection (an amount equal to 17 compared to 10 in scenario 2). Thus, the signaling peak is higher. In scenario 6a, one preconditioning dose of an amount equal to 2 is applied at t=0 (dotted line). This regimen results in two signaling peaks with a higher second peak. We note that the magnitude of the second peak is slightly smaller than the peak in the non-preconditioned system. If the amount of the initial LPS stimulus is equal to 5, then the second LPS peak is significantly smaller than the non-preconditioned system (scenario 6b). In fact, the second peak is also smaller than the initial peak. Figure 6B shows that again the magnitude S_{max} of the second peak decreases approximately linearly with the increase in preconditioning until a threshold $A(t=0) \sim 7$ is reached beyond which no further decrease in signaling through preconditioning is achievable. We conclude that preconditioning can help desensitize the LPS effects. We observe tolerance of the system, and the second lethal LPS stimulus is now non-lethal.

Phase diagram—Further visualization of the preconditioning and priming behavior can be obtained by plotting the TLR4-LPS complex (C) versus free TLR4 receptor concentration (R) for cases with and without preconditioning. The standard trajectory, shown as a heavy solid curve in Figure 7, corresponds to initial LPS injection at the level 5. It starts at the point $C = 0$, $R = 4$ and is traversed in counterclockwise direction as indicated by the arrows. If a second LPS injection (of magnitude 10) is administered at time Δt after the first, the trajectory will continue along one of the dashed curves, originating at the appropriate point of the standard trajectory. The peak in signaling will be roughly equal in magnitude of the peak in TLR4-LPS complex and can be determined in the graph as the maximum value of C attained along the trajectory. One observes three distinct regimes in Figure 7: if $\Delta t < 2h$ then the second peak will be larger than the first (corresponding to priming behavior). If $2h < \Delta t < 70h$ then the second peak will be lower than the first peak (although the amount of LPS used in the second injection was larger than in the first). The most optimal separation of the two injections is $\Delta t = 12h$.

DISCUSSION

Sepsis is a state in which runaway inflammation is driven by bacterial infection [28;30] and perpetuated by the body's own alarm/danger response [19;21] The acute inflammatory response to biological stress such as bacterial infection involves a cascade of events mediated by a large array of cells and molecules that locate invading pathogens or damaged tissue, alert and recruit other cells and molecules, eliminate the offending agents, and finally restore the body to equilibrium. This response is accompanied by macroscopic manifestations such as fever and elevated heart rate, which contribute to optimize the various defense mechanisms involved [25]. Much of this response in the setting of sepsis is driven by the bacterial cell wall component LPS, which is now known to signal predominantly via TLR4 [4;20].

One long-studied phenomenon is the paradoxical inability of inflammatory cells derived from the blood of septic patients to produce inflammatory mediators, despite the generally high levels of these same inflammatory in the blood [1;5–7;27;29]. This phenomenon is thought to be the same as LPS tolerance (desensitization), which can be seen both in inflammatory cells *in vitro* as well as at the whole-organism level [6;9;24;37]. Desensitization is only one possible outcome of a broader phenomenon, that of preconditioning (which also involves priming, i.e. the super-induction of inflammatory mediators upon repeated stimulation, often examined *in vitro* in cells such as macrophages [26]). We have developed a series of computational simulations of the whole-organism inflammatory response, in which pro- and anti-inflammatory mediators are induced by infection or sterile trauma and are further modulated by products derived from damaged or dysfunctional tissues [2;33;34]. Using one of these models, we have gained insight into the phenomenon of preconditioning at the whole-animal level [9]. In that study, we utilized a four-dimensional model of this response to reproduce many scenarios involving repeated LPS administration, including both tolerance and potentiation, from a single parameter set under different administration protocols. The key determinants of the outcome of our simulations were the relative timescales of model components, specifically the slower dynamics of the anti-inflammatory mediator with respect to the pro-inflammatory mediator [9].

In the present study, we turned our attention to the study of preconditioning at the cellular level. We hypothesized that preconditioning is inherent to the dynamics of the signaling process. Indeed, prior studies had suggested that desensitization in response to LPS is associated with suppression of TLR4 signaling [13]. We created a simplified model of this process, nominally in macrophages, consisting of LPS (A), TLR4 (R), the bound complex LPS-TLR4 (C), and downstream signaling events (S). Our numerical results show that preconditioning effects depend on the preconditioning amount and on the time interval between the successive

injections. By varying these parameters, we obtain all possible scenarios, namely priming, desensitization and no difference between signaling peaks.

Our results suggest that preconditioning is controlled by the degeneration rate of TLR4, the time interval between repeated LPS stimuli, and the magnitude of each LPS stimulus. We find that following a preconditioning LPS stimulus, the signaling peak driven by a second LPS stimulus decreases approximately linearly with the increase in preconditioning, until a threshold is reached beyond which no further decrease in signaling through preconditioning is achievable. Furthermore, our simulations suggest that as the amount of preconditioning increases, it takes longer for the system to go back to its normal state. Additionally, exposure to several successive preconditioning doses maintains cells in a tolerant (LPS-insensitive) state, with greater tolerance occurring in the presence of fewer successive LPS stimuli vs. more frequent, very small LPS stimuli.

In the case of preconditioning amounts smaller than the amount of LPS stimulus in the non-preconditioned case, we always observe desensitization of the system. In other words, the signaling peaks in preconditioned systems are smaller than in non-preconditioned systems. We also show that there is a threshold amount of preconditioning above which the second signaling peak is no further reduced, in line with published studies [11]. Our simulations also suggest an optimal time interval between doses of LPS (approximately 12 h) for the maximal desensitization to occur. These results are also in agreement with published studies [12;18].

There are several limitations to our study. First, we note that our model is a simple component model and therefore we have constrained ourselves to the abstractions inherent in such a mathematical model. We strove to make the simplest assumptions possible about LPS/TLR4 signaling, in order to see if preconditioning behavior would emerge. Second, we did not include a decay mechanism for LPS, as LPS is known to be intrinsically stable *in vitro* with a negligible death rate (see [14;17]). *In vivo*, the liver is the main organ involved in the clearance of LPS from the bloodstream, which occurs via uptake of LPS [22;32]. To examine the effect of the addition of a nonzero decay rate on our simulations, we re-ran our simulations with a modified model including a death rate for LPS, and we observe that in all cases LPS decays to 0 within the period t = 80h if the value of the death rate is greater than a certain threshold (data not shown). If the death rate is chosen to be very small, the amounts of LPS at t = 80h remain nonzero in the examples of high levels of LPS stimuli. To our knowledge, there is no published literature specifically on the decay kinetics of the molecule, and we believe this is because the binding mechanism is the dominant mechanism in clearance of LPS *in vivo* [22;32]. Third, in our simple model, signaling amplification is achieved simply by changing the value of the signaling rate. By doing so, the resulting signaling curves become more narrow or more spread out without altering the interpretation of the results (data not shown). While we acknowledge that more sophisticated treatments of signaling amplification might be modeled, this would greatly expand the size and scope of our model and require us to increase the complexity of other aspects of the model correspondingly.

We suggest that the studies we carried out herein have a broader applicability to the study of preconditioning in other aspects of inflammation. Toll-like receptor 4 recognizes so-called pathogen-associated molecular patterns (e.g. LPS) [4;20], but this receptor also recognizes damage-associated molecular patterns (e.g. the DNA binding alarmin HMGB1 [3;8;10;35;36], and, hence, appears to be centrally involved in the immune response during both infection and injury [23]. Importantly, HMGB1 appears to mediate preconditioning via TLR4 [15;16]. Thus, expansion of the present studies with parameters relevant to the interaction between HMGB1 and TLR4 may yield important insights into the phenomenon of cross-tolerance (i.e. preconditioning in settings of stimulation with heterogeneous stimuli [6;37]).

In summary, the studies presented herein suggest that the features inherent to a relatively simple signaling cascade involving LPS and TLR4 can explain many of the phenotypes associated with preconditioning. We suggest that this phenomenon may be an evolved feature of the inflammatory cascade, presumably to allow both rapid ramp-up of inflammation (priming) as well as resolution (desensitization).

Acknowledgements

This work was supported by National Institutes of Health grants P50-GM-53789-08 (YV, BR), R01-HL080926 (YV), and R33-HL-089082. DS acknowledges support by Alfred P. Sloan Foundation.

ABBREVIATIONS

LPS
: bacterial lipopolysaccharide

TLR
: Toll-like receptor

References

1. Adrie C, Pinsky MR. The inflammatory balance in human sepsis. Intensive Care Med 2000;26:364–375. [PubMed: 10872127]
2. An, G.; Mi, Q.; Bartels, J.; Chang, S.; Vodovotz, Y. Computational Models of Inflammation: Applications to Sepsis, Trauma, and Tissue Healing. In: Villoslada, P.; Cascante, M., editors. Systems Biology in Medicine. Humana Press; Totowa, NJ: 2008. In Press
3. Andersson U, Erlandsson-Harris H, Yang H, Tracey KJ. HMGB1 as a DNA-binding cytokine. J Leukoc Biol 2002;72:1084–1091. [PubMed: 12488489]
4. Beutler B. Innate immunity: an overview. Mol Immunol 2004;40:845–859. [PubMed: 14698223]
5. Cavaillon JM, Adrie C, Fitting C, dib-Conquy M. Reprogramming of circulatory cells in sepsis and SIRS. J Endotoxin Res 2005;11:311–320. [PubMed: 16263005]
6. Cavaillon JM, Adrie C, Fitting C, dib-Conquy M. Endotoxin tolerance: is there a clinical relevance? J Endotoxin Res 2003;9:101–107. [PubMed: 12803883]
7. Cavaillon JM, dib-Conquy M. Determining the degree of immunodysregulation in sepsis. Contrib Nephrol 2007;156:101–111. [PubMed: 17464119]
8. Czura CJ, Wang H, Tracey KJ. Dual roles for HMGB1: DNA binding and cytokine. J Endotoxin Res 2001;7:315–321. [PubMed: 11717586]
9. Day J, Rubin J, Vodovotz Y, Chow CC, Reynolds A, Clermont G. A reduced mathematical model of the acute inflammatory response: II. Capturing scenarios of repeated endotoxin administration. J Theor Biol 2006;242:237–256. [PubMed: 16616206]
10. Erlandsson HH, Andersson U. Mini-review: The nuclear protein HMGB1 as a proinflammatory mediator. Eur J Immunol 2004;34:1503–1512. [PubMed: 15162419]
11. Fahmi H, Chaby R. Desensitization of macrophages to endotoxin effects is not correlated with a down-regulation of lipopolysaccharide-binding sites. Cell Immunol 1993;150:219–229. [PubMed: 7688269]
12. Fahmi H, Chaby R. Selective refractoriness of macrophages to endotoxin-induced production of tumor necrosis factor, elicited by an autocrine mechanism. J Leukoc Biol 1993;53:45–52. [PubMed: 8426091]
13. Fan H, Cook JA. Molecular mechanisms of endotoxin tolerance. J Endotoxin Res 2004;10:71–84. [PubMed: 15119998]
14. Fox ES, Thomas P, Broitman SA. Comparative studies of endotoxin uptake by isolated rat Kupffer and peritoneal cells. Infect Immun 1987;55:2962–2966. [PubMed: 2824379]

15. Izuishi K, Tsung A, Jeyabalan G, Critchlow ND, Li J, Tracey KJ, DeMarco RA, Lotze MT, Fink MP, Geller DA, Billiar TR. Cutting edge: high-mobility group box 1 preconditioning protects against liver ischemia-reperfusion injury. J Immunol 2006;176:7154–7158. [PubMed: 16751357]
16. Klune JR, Billiar TR, Tsung A. HMGB1 preconditioning: therapeutic application for a danger signal? J Leukoc Biol 2008;83:558–563. [PubMed: 17938274]
17. Lachmann U, Schmidt W, Wunderlich H, Schafer H. Radioiodination of S-type lipopolysaccharide. Possibilities and limitations of labelling of the carbohydrate chain by periodate oxidation. Zentralbl Bakteriol 1992;276:313–322. [PubMed: 1315597]
18. Marchant A, Gueydan C, Houzet L, Amraoui Z, Sels A, Huez G, Goldman M, Kruys V. Defective translation of tumor necrosis factor mRNA in lipopolysaccharide-tolerant macrophages. J Inflamm 1996;46:114–123. [PubMed: 8734792]
19. Matzinger P. The danger model: a renewed sense of self. Science 2002;296:301–305. [PubMed: 11951032]
20. Means TK, Golenbock DT, Fenton MJ. The biology of Toll-like receptors. Cytokine Growth Factor Rev 2000;11:219–232. [PubMed: 10817965]
21. Medzhitov R, Janeway C Jr. Innate immunity [Review]. N Engl J Med 2000;343:338–344. [PubMed: 10922424]
22. Mimura Y, Sakisaka S, Harada M, Sata M, Tanikawa K. Role of hepatocytes in direct clearance of lipopolysaccharide in rats. Gastroenterology 1995;109:1969–1976. [PubMed: 7498663]
23. Mollen KP, Anand RJ, Tsung A, Prince JM, Levy RM, Billiar TR. Emerging paradigm: toll-like receptor 4-sentinel for the detection of tissue damage. Shock 2006;26:430–437. [PubMed: 17047512]
24. Munoz C, Carlet J, Fitting C, Misset B, Bleriot JP, Cavaillon JM. Dysregulation of in vitro cytokine production by monocytes during sepsis. J Clin Invest 1991;88:1747–1754. [PubMed: 1939659]
25. Nathan C. Points of control in inflammation. Nature 2002;420:846–852. [PubMed: 12490957]
26. Nathan C. Mechanisms and modulation of macrophage activation. Behring Inst Res Commun 1991;88:200–207.
27. Pinsky MR. Sepsis: a pro- and anti-inflammatory disequilibrium syndrome. Contrib Nephrol 2001:354–366. [PubMed: 11395903]
28. Pinsky MR. Sepsis and multiple organ failure. Contrib Nephrol 2007;156:47–63. [PubMed: 17464115]
29. Pinsky MR. Dysregulation of the immune response in severe sepsis. Am J Med Sci 2004;328:220–229. [PubMed: 15486537]
30. Rice TW, Bernard GR. Therapeutic intervention and targets for sepsis. Annu Rev Med 2005;56:225–248. [PubMed: 15660511]
31. Shin HJ, Lee H, Park JD, Hyun HC, Sohn HO, Lee DW, Kim YS. Kinetics of binding of LPS to recombinant CD14, TLR4, and MD-2 proteins. Mol Cells 2007;24:119–124. [PubMed: 17846506]
32. Su GL, Dorko K, Strom SC, Nussler AK, Wang SC. CD14 expression and production by human hepatocytes. J Hepatol 1999;31:435–442. [PubMed: 10488701]
33. Vodovotz Y. Deciphering the complexity of acute inflammation using mathematical models. Immunologic Res 2006;36:237–246.
34. Vodovotz Y, Csete M, Bartels J, Chang S, An G. Translational systems biology of inflammation. PLoS Comput Biol 2008;4:1–6.
35. Wang H, Yang H, Czura CJ, Sama AE, Tracey KJ. HMGB1 as a late mediator of lethal systemic inflammation. Am J Respir Crit Care Med 2001;164:1768–1773. [PubMed: 11734424]
36. Wang H, Yang H, Tracey KJ. Extracellular role of HMGB1 in inflammation and sepsis. J Intern Med 2004;255:320–331. [PubMed: 14871456]
37. West MA, Heagy W. Endotoxin tolerance: a review. Crit Care Med 2002;30:S64–S73.

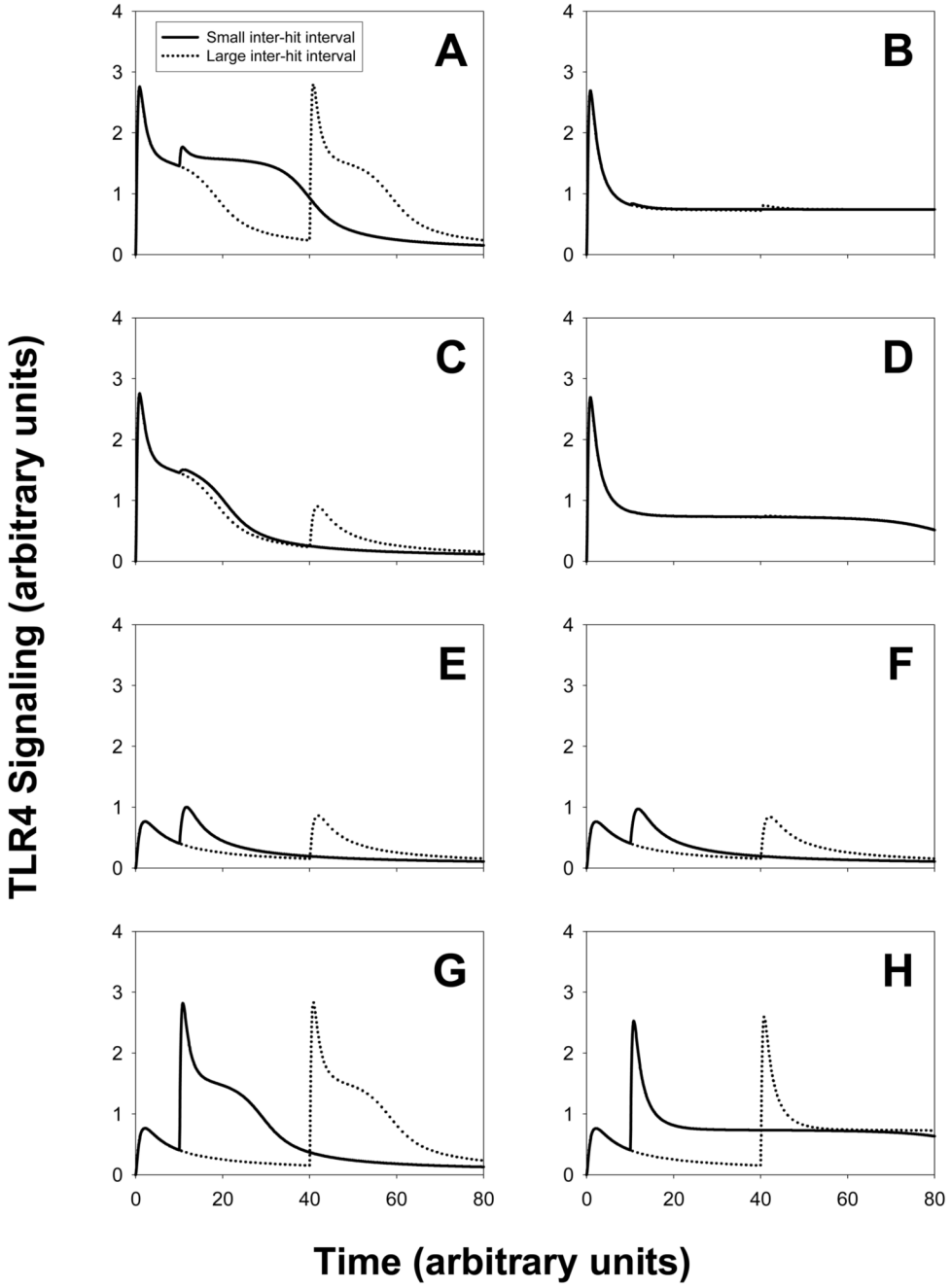

Figure 1. Scenario 1: Signaling amounts versus time

Panels A, C, E and G correspond to a rate of expression of receptors that is five times larger than the rate in panels B, D, F and H. One injection of LPS is done at the initial time t=0 and a second injection of LPS occurs at a later time t= Δt. The solid curves result from a small time interval whereas the dotted curves result from a large time interval Δt (four times larger). Comparing figures from the right column to the left column shows that the expression rate of receptors has an influence on the magnitude of the second signaling peak. The amount of LPS injected varies: two large equal amounts (panel A,B); one large followed by one small amount (panel C, D); two small equal amounts (panel E, F); one small followed by one large amount (panel G,H).

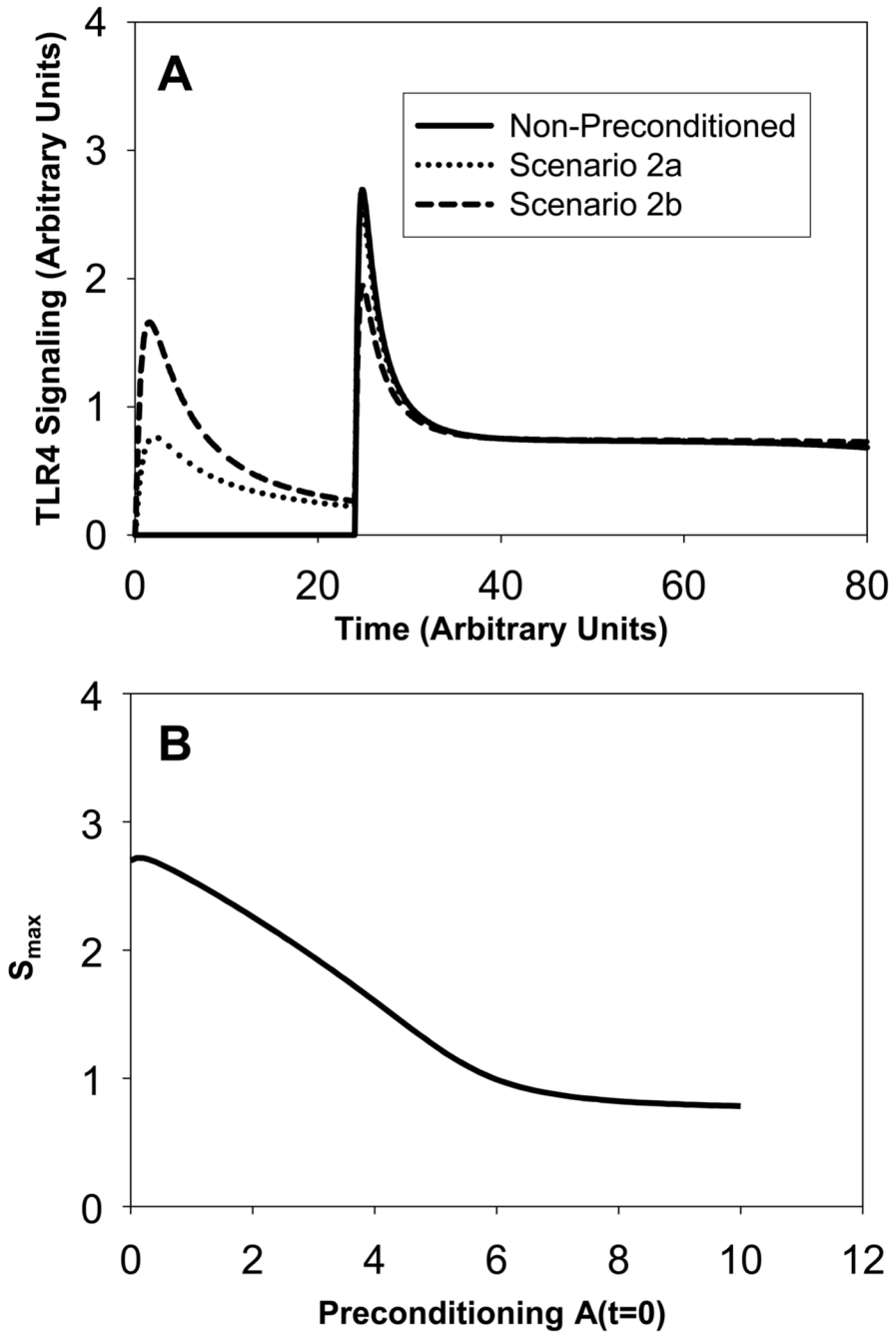

Figure 2. Scenario 2: Signaling amounts versus time

Panel A: The solid curve shows the non-preconditioned signaling. As we increase the amount of preconditioning (amount equal to 1 for dotted curve and amount equal to 3 for dashed curve), the magnitude of the signaling peak for the second large LPS stimulus decreases. . Panel B: The magnitude S_{max} of the second peak in TLR4 signaling versus the amount of preconditioning A(t=0).

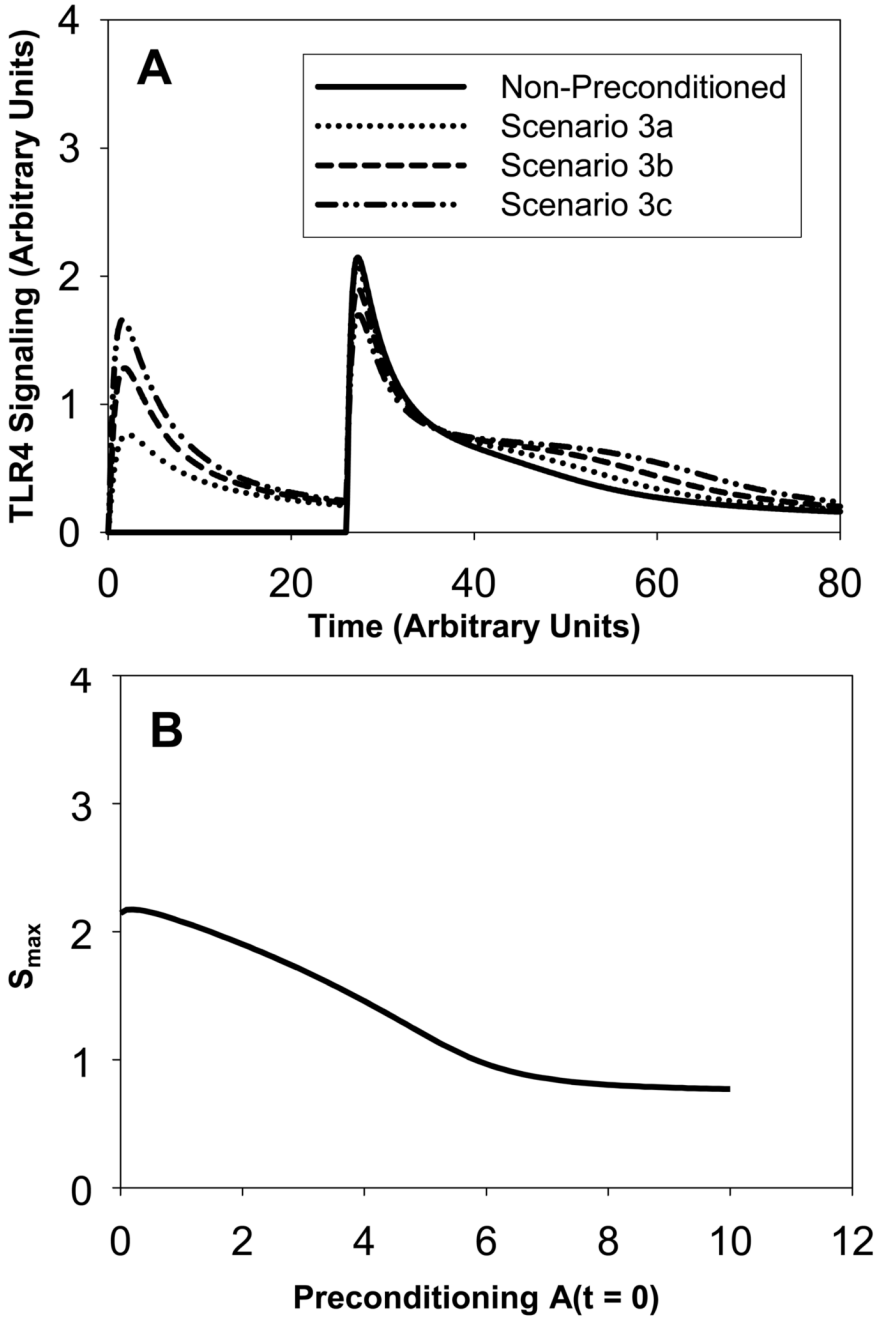

Figure 3. Scenario 3: Signaling amounts versus time

Panel A: The solid curve corresponds to no preconditioning. As in Scenario 2, the magnitude of the second peak in the preconditioned system decreases as the amount of LPS for the first stimulus increases. The dotted curve corresponds to a preconditioning amount of 1 at time t=0h. The dashed curve corresponds to a preconditioning amount of 2 at time t=0h. The dash-dot-dot curve corresponds to a preconditioning amount of 3 at time t=0h. In the latter case, we observe a second peak of same magnitude even though the second stimulus corresponds to a larger amount (equal to 5). We also note that the peak decreases but the "tail becomes larger". Panel B: The magnitude S_{max} of the second peak in TLR4 signaling versus the amount of preconditioning A(t=0).

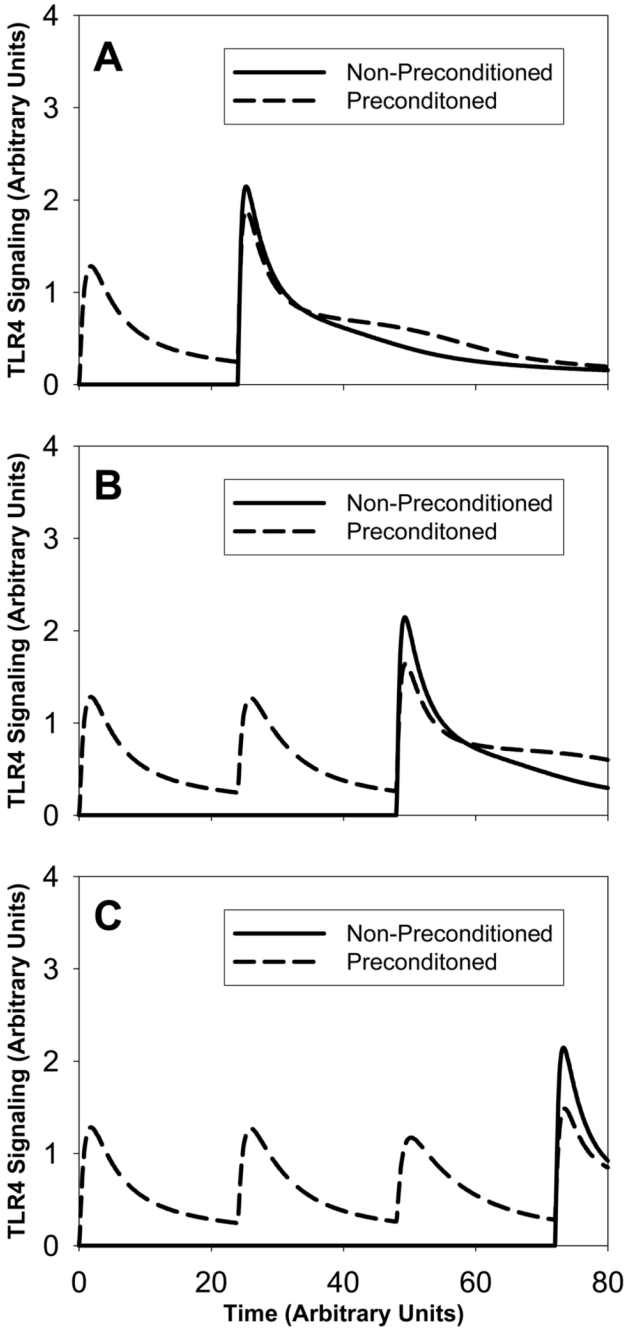

Figure 4. Scenario 4: Signaling amounts versus time

The solid lines correspond to no-preconditioned systems and the dashed lines correspond to preconditioned systems in panels A, B and C. We vary the number of LPS preconditioning stimuli of equal amount: one in panel A, two in panel B and three in panel C. We observe that as we increase the number of successive small amount of preconditioning, the resulting signaling peak decreases.

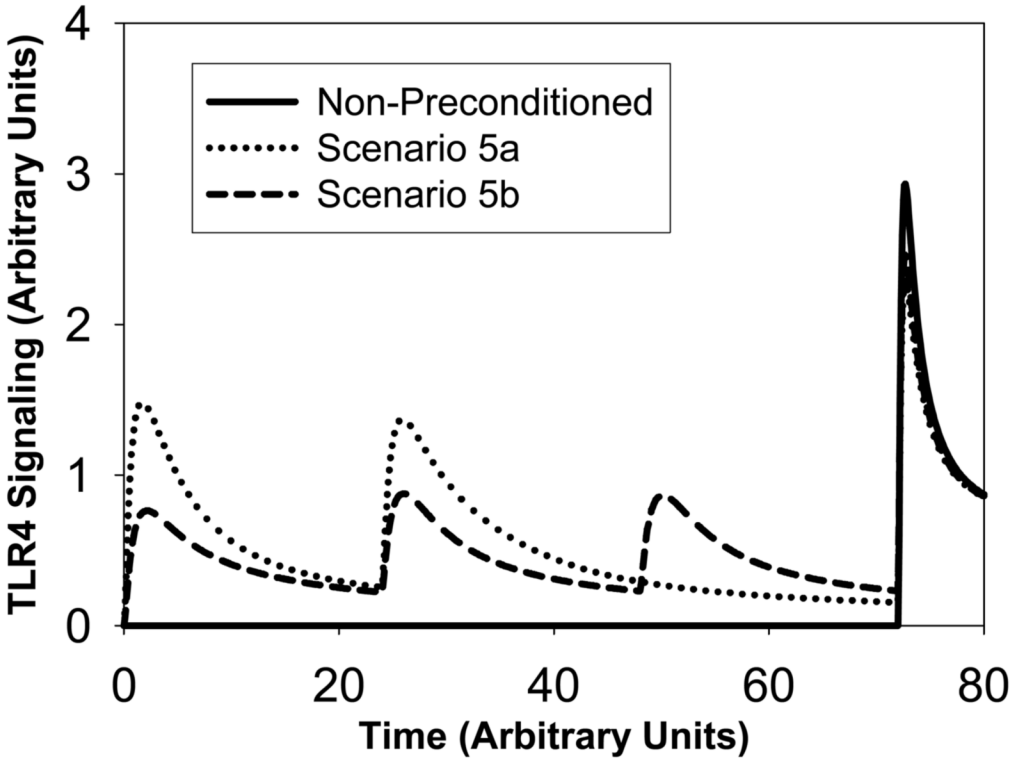

Figure 5. Scenario 5: Signaling amounts versus time

The solid curve corresponds to no-preconditioned system. The dotted curve corresponds to two stimuli of an amount equal to 2.5 whereas the dashed curve corresponds to three successive stimuli of a smaller amount equal to 1. The resulting dashed peak is however slightly larger than the resulting dotted signaling peak.

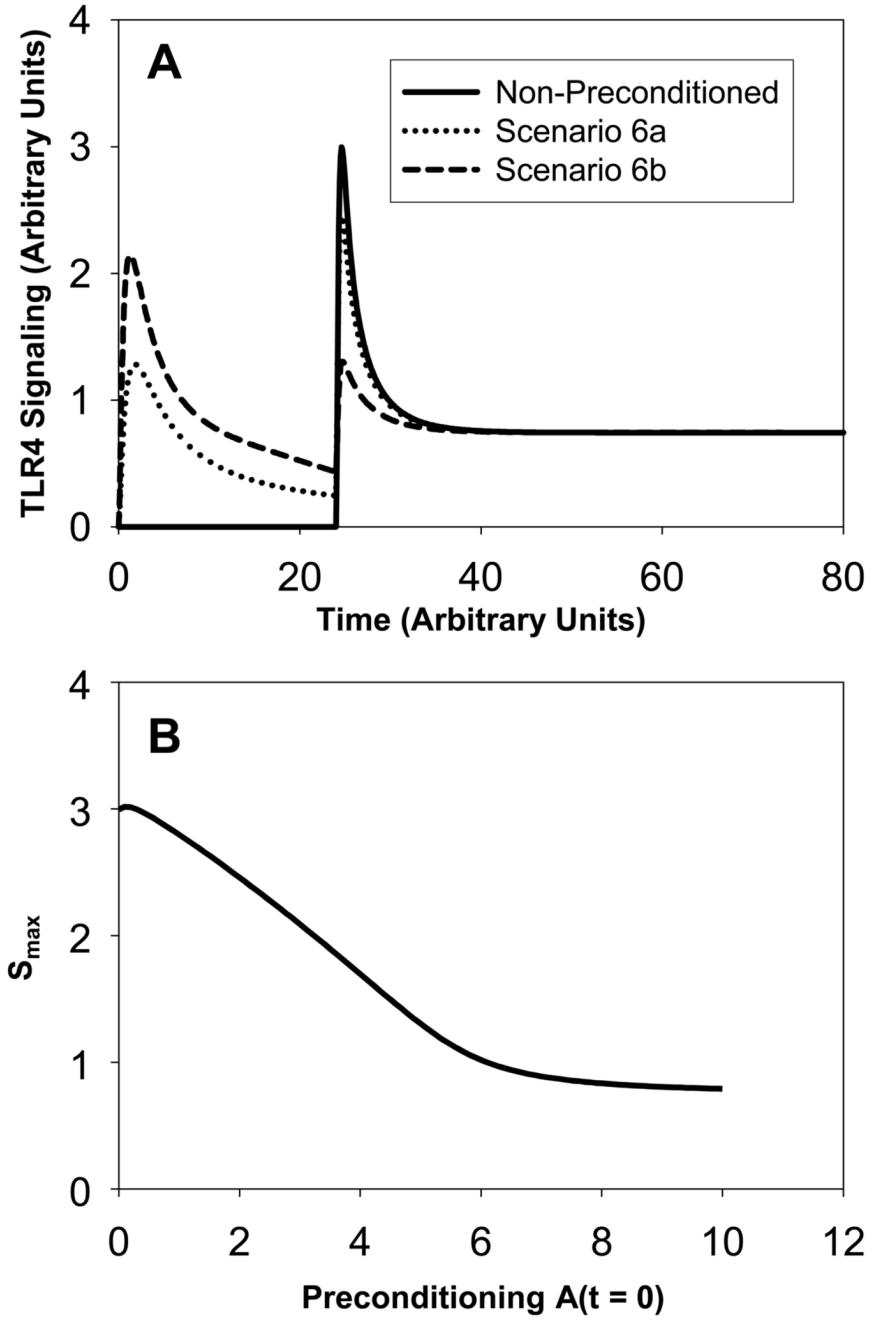

Figure 6. Scenario 6: Signaling amounts versus time

Panel A: The solid curve corresponds to no-preconditioned system. The dotted curve corresponds to a small amount of preconditioning (equal to 2) and the dashed curve to a larger amount of preconditioning (equal to 5). The dotted curve shows priming whereas the dashed curve shows desensitization. Panel B: The magnitude S_{max} of the second peak in TLR4 signaling versus the amount of preconditioning A(t=0).

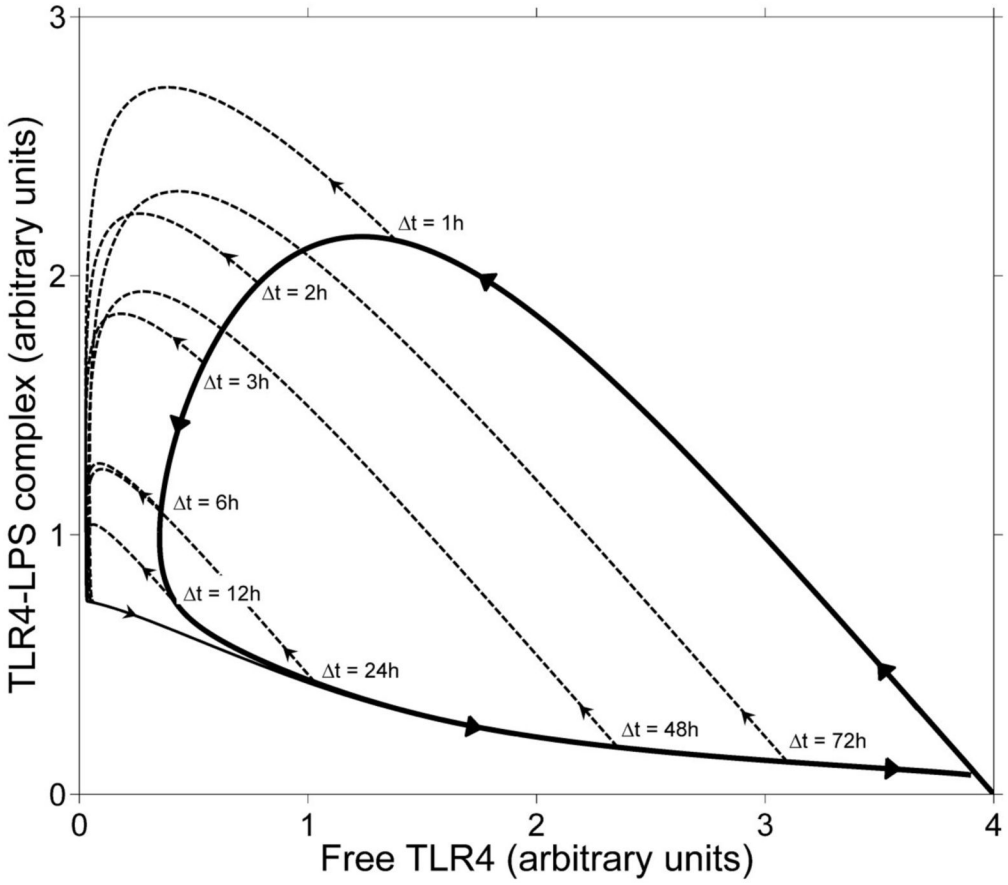

Figure 7. Phase diagram of preconditioning

The solid curve shows the trajectory of a simple scenario with one injection of LPS of magnitude 5. The dashed curves show the trajectory of a scenario in which a second injection of magnitude 10 follows Δ*t* hours after the first injection. The local maxima of TLR4-LPS complex correspond to peaks in the signaling.

Table 1

parameters for mathematical model

All parameters are in arbitrary units. Where possible, parameter values were calculated from the literature as indicated.

Rate	Value
Binding reaction rate (k1)	0.33 (From Ref. 28)
Internalization rate (k3)	0.2
Signaling rate (k4)	10
Receptor regeneration rate (k2)	0.1 or 0.5
Inverse binding rate k_{-1}	1.e-7 (From Ref. 28)
Initial amount of free receptors R(t=0)	4
Limiting amount of free receptors r_0	4
Initial amount of complex C(t=0)	0
Internalization threshold value c_0	0.04

Table 2

parameters for scenarios

	A(t=t1)	*t1*	*A(t=t2)*	*t2*	*A(t=t3)*	*t3*	*A(t=t4)*	*t4*
Scenario 2								
Non-preconditioned	0	0	10	24				
Preconditioned 2a	1	0	10	24				
Preconditioned 2b	3	0	10	24				
Scenario 3								
Non-preconditioned	0	0	5	26				
Preconditioned 3a	1	0	5	26				
Preconditioned 3b	2	0	5	26				
Preconditioned 3c	3	0	5	26				
Scenario 4								
Non-preconditioned 4a	0	0	5	24				
Preconditioned 4a	2	0	5	24				
Non-preconditioned 4b	0	0	0	24	5	48		
Preconditioned 4b	2	0	2	24	5	48		
Non-preconditioned 4c	0	0	0	24	0	48	5	72
Preconditioned 4c	2	0	2	24	2	48	5	72
Scenario 5								
Non-preconditioned	0	0	0	24	15	72		
Preconditioned 5a	2.5	0	2.5	24	15	72		
Preconditioned 5b	1	0	1	24	1	48	15	72
Scenario 6								
Non-preconditioned	0	0	17	24				
Preconditioned 6a	2	0	17	24				
Preconditioned 6b	5	0	17	24				